



## Durability of Supersulphated Cement Pastes Activated with Portland Cement in Magnesium Chloride Solution



A. A. Hegazy<sup>1\*</sup>, A. A. Khalil<sup>1</sup>, E. A. El-Alfi<sup>1</sup>, M. F. El-Shahat<sup>2</sup>

<sup>1</sup>Refractories, Ceramics and Building Materials Department, National Research Centre, Cairo, Egypt.

<sup>2</sup>Chemistry Dept., Faculty of Science, Ain Shams University, Cairo, Egypt.

**T**HIS STUDY investigates the effect of chemical attack of chlorides on the physicochemical properties of the prepared supersulphated cement (SSC) pastes activated by 2-11 % ordinary Portland cement (OPC) after immersion in 4% magnesium chloride solution for up to 12 months. Results indicated that the bulk density increases while the apparent porosity decreases with hydration time for all the SSC pastes. The compressive strength results showed a significant increase for all SSC samples hydrated up to 12 months whereas they showed high resistance to deterioration. The hydration products appeared via XRD, FTIR, TG, DTG, and DSC are ettringite, gypsum, anhydrite, and calcium silicate hydrate (CSH).

**Keywords:** Supersulphated cement, Slag, Anhydrite, Physicochemical properties, Magnesium chloride, Aggressive media.

### Introduction

Concrete is the most widely used material in construction due to its versatility whereas it can be easily molded into any desired shape or form [1]. Moreover, fresh concrete forms a highly alkaline environment that protects the reinforced iron bars (rebars) in structural concrete from corrosion mainly due to the presence of an oxides layer known as (passive film) composed of a dense ferrous (Fe<sup>+2</sup>) and/or ferric (Fe<sup>+3</sup>) that prevents further oxidization of the iron bars [2]. In spite of the advantages of concrete, it has two main drawbacks represented in the huge amount of emitted carbon dioxide during manufacturing and the durability of concrete in aggressive media containing sulphate or chloride ions.

Firstly, the main ingredient in the production of concrete which is ordinary Portland cement (OPC) which accounts for approximately 7% of global carbon dioxide (CO<sub>2</sub>) emissions [3]. Portland cement manufacturing consumes huge

amount of energy represents approximately 2–3% of the global primary energy use. Most of the energy used in Portland cement manufacture is heat required for clinker formation, i.e. the decarbonation of limestone and the reaction of the resulted lime with the other ingredients, such as clay minerals [4]. Furthermore, each produced ton of Portland cement results in approximately 0.87 ton of carbon dioxide gas which is one of several gases that are responsible for the green house effect, and thus have the potential to increase average global temperatures. [4, 5].

On the other hand, concrete made of Ordinary Portland cement has low durability in the presence of chlorides or sulphates found in soil or underground water. Chloride ions interact with the hydration products of Tricalcium Aluminate (C<sub>3</sub>A) and Tetracalcium Aluminoferrite (C<sub>4</sub>AF) phases of OPC, for instance, to form

$3\text{CaO}\cdot\text{Al}_2\text{O}_3\cdot\text{CaCl}_2\cdot 10\text{H}_2\text{O}$  (Friedel's salt) and  $3\text{CaO}\cdot\text{Fe}_2\text{O}_3\cdot\text{CaCl}_2\cdot 10\text{H}_2\text{O}$ , respectively [6] which

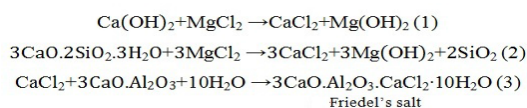
\*Corresponding author e-mail: dr.ahgazy@yahoo.com

Received 31/12/2018, Accepted 14/1/2019

DOI: 10.21608/ejchem.2019.6563.1579

©2019 National Information and Documentation Center (NIDOC)

cause softening to the concrete, as indicated from the following equations:



Additionally, the ingress of chloride ions to the steel surface is the most important cause of corrosion initiation of steel bar [7-10]. Corrosion of steel bar as well as the softening of the concrete has a synergetic effect on the deterioration of the reinforced concrete structures. Corrosion of the steel bars reduces its cross-sectional size and produces corrosion products with a larger volume than the steel itself which results in cracking and eventual structural failure [11,12].

In an attempt to overcome these problems, researchers focused on new cement binding materials as alternatives to OPC [13, 14]. This respect is mainly based on using supplementary cementitious materials (SCM) such as ground granulated blast furnace slag (GGBS), fly ash, silica fume, meta-kaolin... etc to partially substitute Portland cement in the making concrete to reduce consumed energy and save raw materials. The use of (GGBS) as supplementary cementitious material improves the durability of concrete as it reduces the chloride penetration which has been mentioned by different investigators [15, 16].

In this study slag is used as a main ingredient of an alternative binding material which is supersulphated cement (SSC). Supersulphated cements are binders free (or almost free) of Portland cement clinker. It was reported that they almost consist of (80:15:5) of (slag: anhydrite: alkaline activator) respectively. Moreover, it was added that the slag content of this cement could be  $\geq 75\%$  [17, 18]. The prepared SSC pastes will be tested for durability in magnesium chloride solution to correlate the percentage of the added OPC to the physicomechanical properties as well as the phase structure.

## Materials and Methods

### Materials

The starting materials were blast furnace slag that was supplied by the iron and steel factory located in Helwan province, Egypt, which was ground in a steel ball mill to a Blaine surface area of 4500 cm<sup>2</sup>/g. Anhydrite, on the other hand, was

prepared by heating local pure gypsum ore (Ras Malaab, Sinai) at 750° C while OPC is a CEM I class 42.5 N.

### Methods

The starting materials were chemically analyzed, using the Axios WD XRF sequential spectrometer (PANalytical, 2005) spectrometry. The obtained results of the chemical composition presented in Table 1 were used to design the mix composition that is given in Table 2. For each mix, the slag, anhydrite and OPC were dry mechanically mixed for 1 h in a ball mill to attain complete homogeneity.

Each mix is blended with the determined amount of normal consistency water to form paste then molded in 2.5 cm cubic moulds and were left for 24 hours in humidity chamber followed by demoulding and curing under water for 28 days (zero time) then transferred to 4% Magnesium Chloride solution to be tested for bulk density, porosity and compressive strength after different hydration times of 1, 3, 6, 9 and 12 months. The test results are expressed as the arithmetic mean of five values for each test as well as the standard deviation values were calculated. A part of the crushed sample was dried at 105°C in the drier oven for 24 hours to stop hydration and then kept in airtight containers for the phase composition determination using XRD, FTIR and thermogravimetric techniques.

The apparent porosity and bulk density were followed according to the principles of Archimedes using water as immersion medium, Compressive strength was determined using a universal testing machine and the applied load for rupture was recorded and divided by the surface area of each cube according to ASTM C109-02 [19].

The phase composition of the hydrated samples was semi quantitatively performed using (Bruker D8 Advance Bruker AXS, Germany, 2001 XRD) whereas Infrared was followed using (Jasco FTIR 6100 spectrometer) and spectra were collected over a range of 4000-400 cm<sup>-1</sup>, using a spectral resolution 4 cm<sup>-1</sup>. While, The DTA–DSC test was performed by using an adaptation of the ASTM E1131: 2008 standard, on thermogravimetric and compositional analysis

of solids and liquids. The equipment used was the simultaneous thermal analyser SHEMAZU (TGA – 50) themogravimetric with a balance

**TABLE 1. Chemical composition of the starting materials.**

Oxides	Slag	OPC	Anhydrite
SiO <sub>2</sub>	33.71	19.52	0.40
TiO <sub>2</sub>	0.61	0.51	—
Al <sub>2</sub> O <sub>3</sub>	8.56	5.66	0.18
MnO	4.85	0.06	—
Fe <sub>2</sub> O <sub>3</sub>	1.43	3.92	0.06
MgO	4.65	2.39	0.15
CaO	36.04	62.05	39.24
Na <sub>2</sub> O	1.33	0.13	0.06
K <sub>2</sub> O	0.94	0.17	0.01
P <sub>2</sub> O <sub>5</sub>	0.02	0.19	0.01
SO <sub>3</sub>	3.08	3.14	57.53
BaO	4.53	0.46	—
SrO	0.13	0.46	0.33
LOI	—	0.96	1.80
Total	99.88	99.62	99.76

**TABLE 2. Mix proportion of the prepared SSC cements.**

Sample	Slag	Anhydrite	OPC
A	83	15	2
B	80	15	5
C	77	15	8
D	74	15	11

accurate to 0.1 mg.

## Results and Discussion

It is planned to discuss the durability of the prepared (SSC) in magnesium chloride solution via measuring the physicomechanical properties including apparent porosity, bulk density, and compressive strength. Moreover, the developed phases were also identified by using XRD, FTIR spectroscopy, TG, DSC and DTG tools of investigations.

### Physicomechanical Properties

#### Apparent Porosity

Generally, the apparent porosity (AP) of cement originated from the elimination of the excess water of workability, used for homogenous mixing of the pastes. It was mentioned that the formed pores are of the open capillary type which is usually filled by the available liquid water of workability.

The apparent porosity (AP) of the SSC cement immersed in magnesium chloride solution is given, as a function of curing time, in Fig. 1. The graph showed a general trend of decrease of the AP values over time. This decrease was due to the mutual precipitation of the hydration products filling such created pores. The precipitation of the hydrated products almost compensates the pores creation.

AP decreases with the time as the hydration proceeds, the decrease was sharp at early ages due to the high rate of the hydration reaction and as the hydration proceeds the pores are filled with

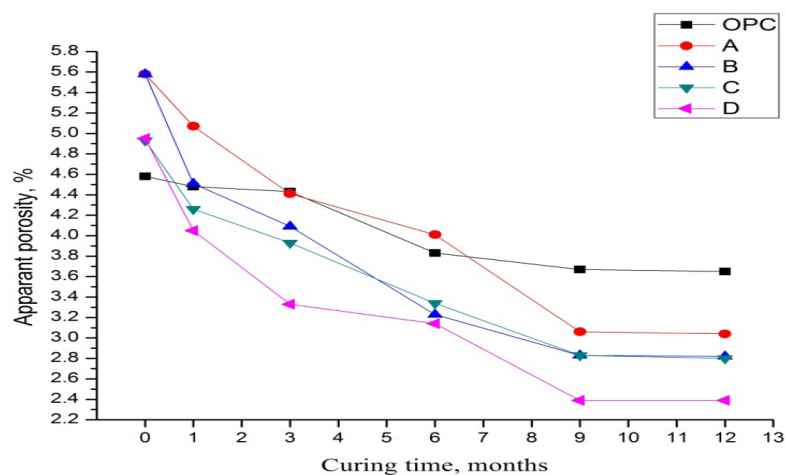


**Fig. 1. The apparent porosity of SSC pastes immersed in 4% MgCl<sub>2</sub> for up to 12 months. (The standard deviation values is between 0.87 to 1.96).**

hydration products and the AP values decrease smoothly. AP decreases also with the increase of OPC content due to the fact that OPC act as an activator for the hydration of slag thus producing more hydration products that fill the pores.

#### *Bulk density (BD)*

The bulk density of the hydrated SSC pastes, as a function of curing time up to 12 months, in 4 %  $\text{MgCl}_2$  solution is graphically presented in Fig. 2 from which it is clear that the BD of the SSC samples increases with curing time for all hydrated pastes in the same time the porosity decrease, as shown previously, due to progress of hydration and mutual precipitation of the hydration products in the originally water filled-spaces constituting the capillary pores of the pastes.

The bulk density of the SSC pastes increased with the Portland cement content due to the fact that OPC act as an activator for the hydration of slag thus producing more hydration products that fill the pores while the cubes almost having the same volume thus the bulk density increases. It is noted that cement A which contains the lowest percentage of OPC showed a slight decrease in the bulk density at later ages of hydration while cement C and D at later ages are almost the same with the higher bulk density values.

Moreover, the chloride ion reacts with  $\text{Ca}(\text{OH})_2$  liberated from hydration silicate phases

of OPC producing  $\text{CaCl}_2$  which intern reacts with  $\text{C}_4\text{AH}_{13}$  to give calcium chloroaluminate hydrate which makes softening and causes deterioration of the OPC paste, so its bulk density decreased. This effect is noted after 3 months of curing under magnesium chloride solution.

#### *Compressive strength*

The compressive strength of the hardened SSC pastes immersed in 4 %  $\text{MgCl}_2$  solution, up to 12 months, are graphically plotted, as function of curing time, in Fig. 3 from which it is clear that the compressive strength of the SSC increases on ageing due to the increase of the hydration products especially CSH which is the main source of the strength. The SSC pastes involve two hydration processes, first one is due to the hydration of included OPC which produces CSH and calcium hydroxide. Second one is due to the reaction of the produced calcium hydroxide with the blast furnace slag to produce more hydration products which increase the compressive strength.

While for the OPC paste, the compressive strength increases up to 3 months which may be due to the accelerating effect of magnesium chloride and then decreases gradually afterwards while immersed in  $\text{MgCl}_2$  solution most probably due to the formation of calcium chloroaluminate  $3\text{CaO} \cdot \text{Al}_2\text{O}_3 \cdot \text{CaCl}_2 \cdot 12\text{H}_2\text{O}$  which softens of the OPC pastes.

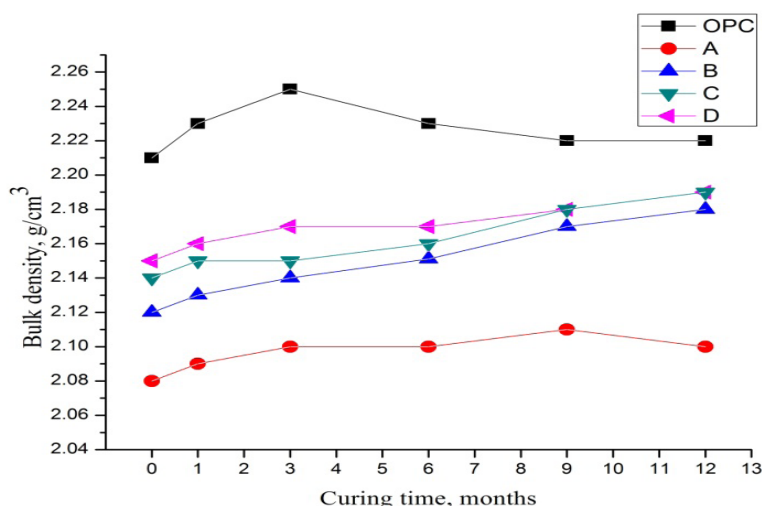


**Fig. 2.** The bulk density of SSC pastes immersed in 4 %  $\text{MgCl}_2$  solution, presented as a function of curing time, up to 12 months. (The standard deviation values is between 0.92 to 1.91).

### Phase composition

#### X-Ray Diffraction (XRD)

XRD patterns of the hardened SSC samples B and D immersed in 4%  $MgCl_2$  solution for 1, 3, 6, and 12 months in addition to the zero time sample are given in Fig. 4 and 5 from which it is clear that the main identified phases are ettringite, anhydrite and gypsum while the presence of CSH and hydrotoalcite-like phases may be overlapped by the gypsum peaks [20].

As the hydration proceeds, the peaks of CSH,

gypsum and ettringite increase while that of the anhydrite diminishes because the hydration of SSC involves the reaction of calcium hydroxide liberated from the alkaline activator (OPC) with slag and anhydrite to produce ettringite and CSH binding phases. Moreover, the zero time sample in both B and D mixes shows a significant peak of anhydrite at ( $2\theta = 25.44^\circ$ ), This peak is decayed in sample B during hydration while completely diminished in the D sample. This may be attributed to the effect of the increase of the alkaline activator (OPC) which leads to faster

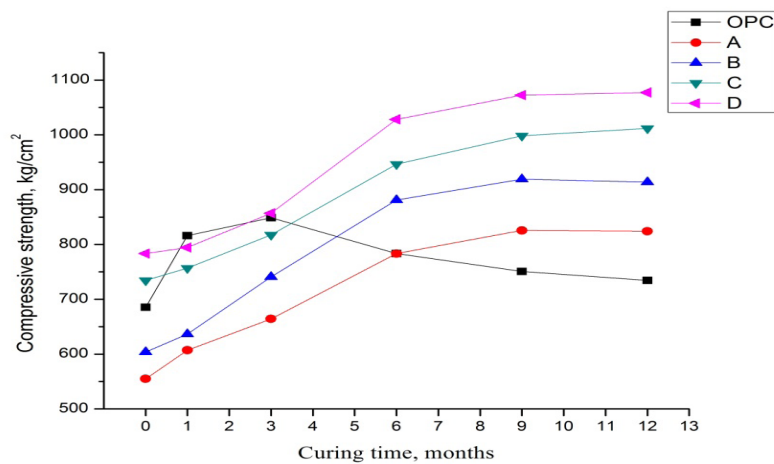


Fig. 3. Compressive strength of hardened SSC pastes immersed in 4% Magnesium chloride solution for up to 12 months. (The standard deviation values is between 0.94 to 2.02)

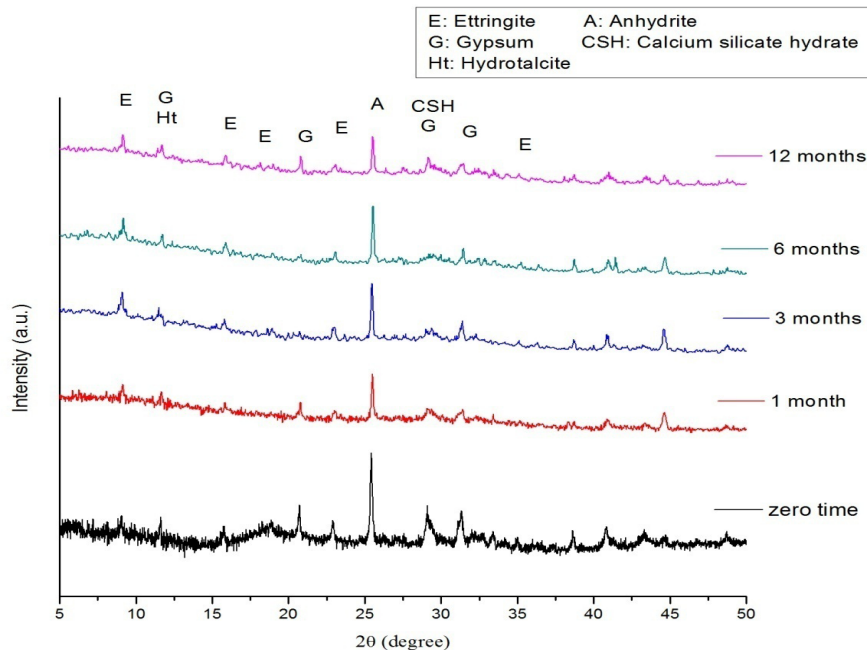


Fig. 4. XRD patterns of SSC (Cement B) pastes immersed in 4%  $MgCl_2$  solution for 12 months.



hydration of slag in the presence of anhydrite to form ettringite and other hydration products.

#### FTIR Spectroscopy

The FTIR spectra of SSC (B and D cements) immersed in 4%  $MgCl_2$ , as a function of curing time, are shown in Fig. 6 and 7 from which it is clear that the band absorbs at about  $3500\text{ cm}^{-1}$  is attributed to a stretching vibration of water bound

in the hydration products while the band at about  $1650\text{ cm}^{-1}$  due to bending vibration of bound water (HOH) [21].

The peaks near  $1450\text{ cm}^{-1}$  are due to C–O stretch of  $CaCO_3$ . A band for S–O stretch occurs near  $1130\text{ cm}^{-1}$  and is partially covered by the Si–O stretch. Moreover it should be noted that ettringite has a single peak at  $1120\text{ cm}^{-1}$  which is

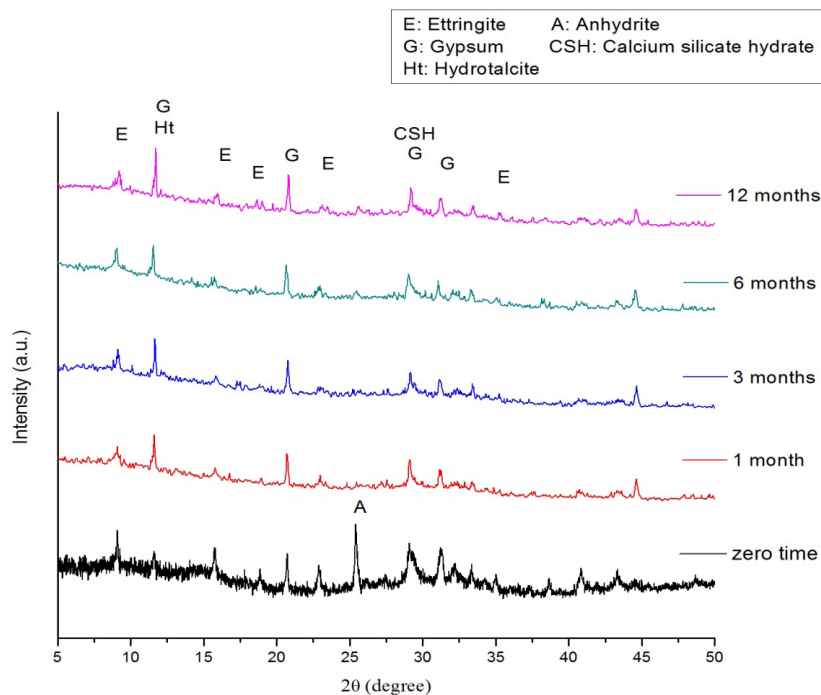


Fig. 5. XRD patterns of SSC (Cement D) pastes immersed in 4%  $MgCl_2$  solution for 12 months.

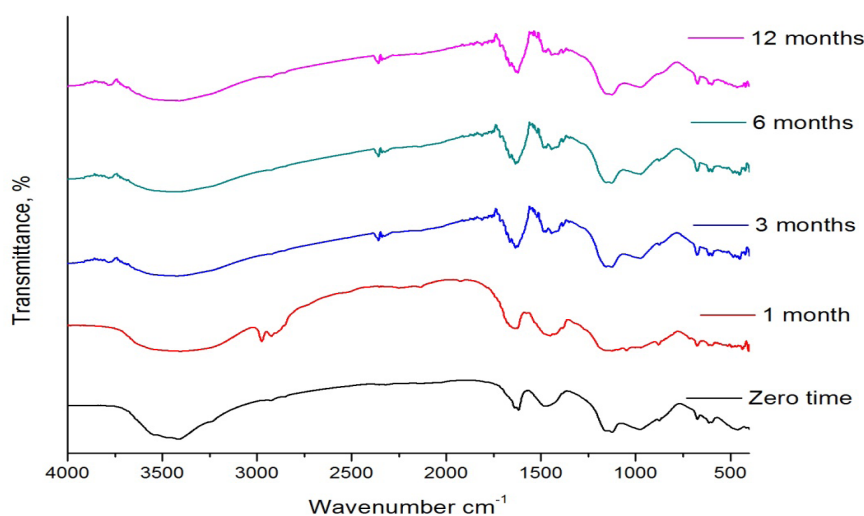


Fig. 6. The FTIR patterns of the B samples cured for up to 12 months in magnesium chloride solution.

in correspondence with the findings of Bensted [22].

In the FTIR graphs it is noted that the band at  $1650\text{ cm}^{-1}$  are getting sharper while that at  $3500\text{ cm}^{-1}$  diminishes by time due to the formation of more hydration products

#### *Thermogravimetric analysis (TG)*

The TG curves of the hydrated SSC pastes (cements B and D) immersed in 4 % magnesium chloride solution for 1, 3, 6 and 12 months are

shown in Fig. 8 and 9. It is clear that the B samples showed 3 steps of weight loss from 25 to 50 °C, from 50 to 98 °C and from 100 to 145 °C while the D samples showed a slightly shifted three steps of weight loss from 25 to 76 °C, from 76 to 104 °C and from 104 to 145 °C. This weight loss is due to the dehydration of the hydration products of SSC pastes which are CSH, ettringite and secondary gypsum. The percentage of weight loss at sample B is 8% while at sample D is 10% which indicates more hydration products in D samples than B ones. Ettringite and CSH are reported to

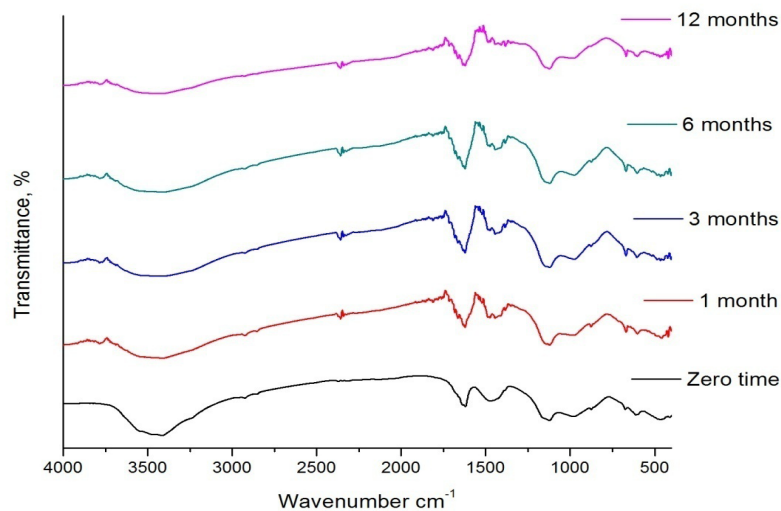


Fig.7. The FTIR patterns of the D samples cured for up to 12 months in magnesium chloride solution.

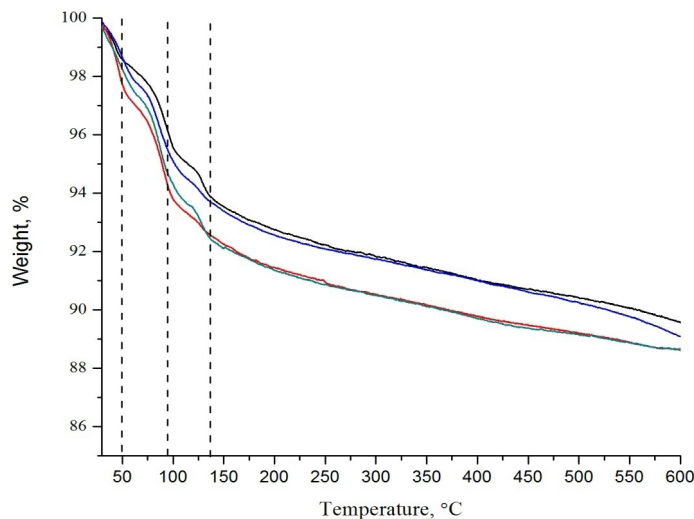


Fig. 8. TG curves of B samples cured in Magnesium chloride solution for 1, 3, 6 and 12 months

dehydrate on heating in the temperature range 90–120 °C, whereas gypsum is reported to dehydrate at approximately 140 °C [23].

*Derivative Thermogravimetric analysis (DTG)*

DTG results of the B and D cement hardened pastes are given in Fig. 10 and 11 from which it is clear that sample B shows a main peak at 90 °C due to the dehydration of CSH and / or ettringite which

increases by aging. This peak is highly announced in the D samples compared with B ones. Moreover, in D samples the main peak is shifted to a higher temperature (102 °C) within hydration time which may be due to the increase in the hydration products and more binding of water to the hydration products producing more crystalline structure as showed in XRD. Moreover, all curves reveal additional peak at about 50 °C which is due to the mechanical held water of the samples.

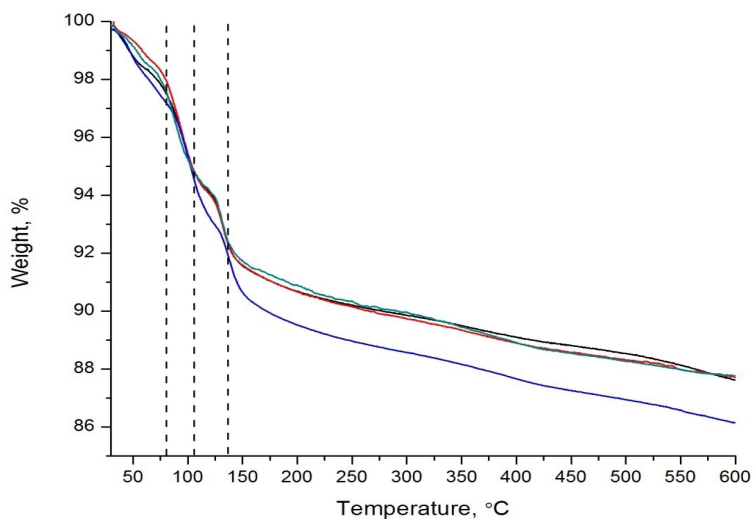


**Fig. 9.** TG curves of D samples cured in Magnesium chloride solution for 1, 3, 6 and 12 months.

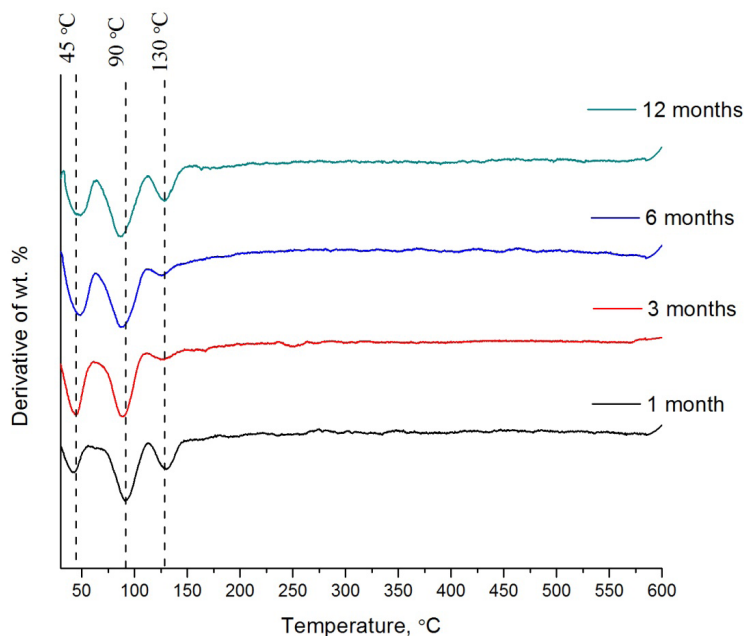


**Fig. 10.** DTG curves of B samples cured in Magnesium chloride solution for 1, 3, 6 and 12 months.



Additionally, a third peak appears at 130 °C at B samples and shifted to 140 °C at D samples which is attributed to gypsum [24].

#### Differential Scanning Calorimetry (DSC)

The DSC graphs of the hydrated (SSC) pastes (cements B and D) cured for 1, 3, 6 and 12 months in 4% magnesium chloride solution are illustrated in Fig. 12 and 13. The endothermic peak appeared at about 100°C in sample B and shifted to 125 °C

in sample D is attributed to the dehydration of calcium silicate hydrate (CSH) and ettringite. The other endothermic peak which appears at 145°C at sample B and shifted to 150°C at sample D is attributed to the dehydration of gypsum. The results show that intensity of CSH and ettringite peaks increase with immersing time, due to the hydration of SSC pastes which produce more hydration products with curing time. Also, the intensity of both peaks increases with increasing

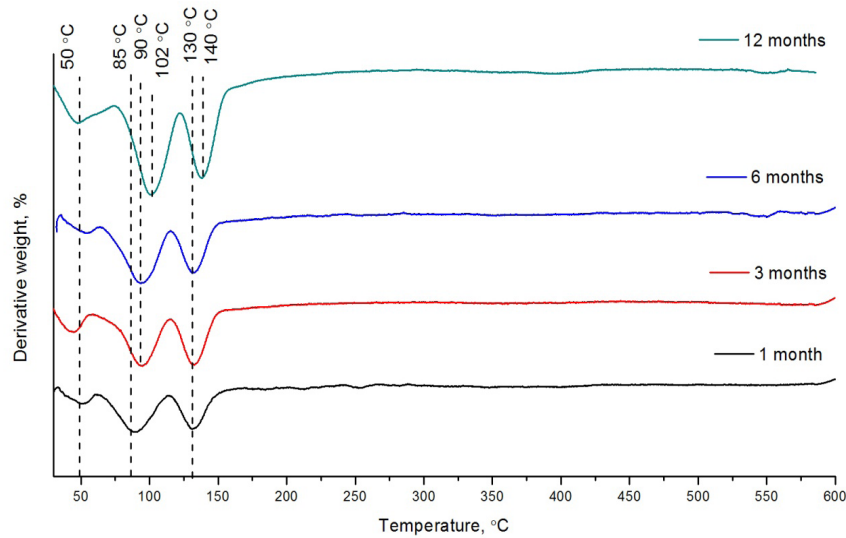


Fig. 11. DTG curves of D samples cured in Magnesium chloride solution for 1, 3, 6 and 12 months.

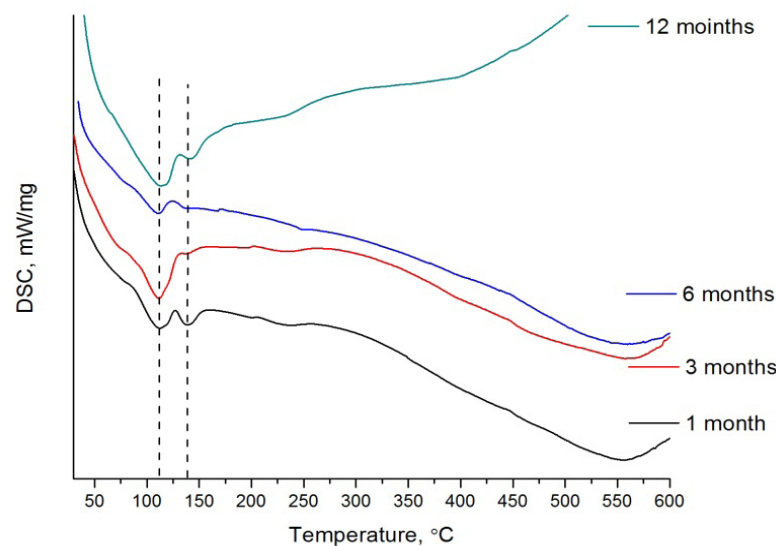


Fig. 12. DSC curves of B samples cured in Magnesium Chloride solution for 1, 3, 6 and 12 months.

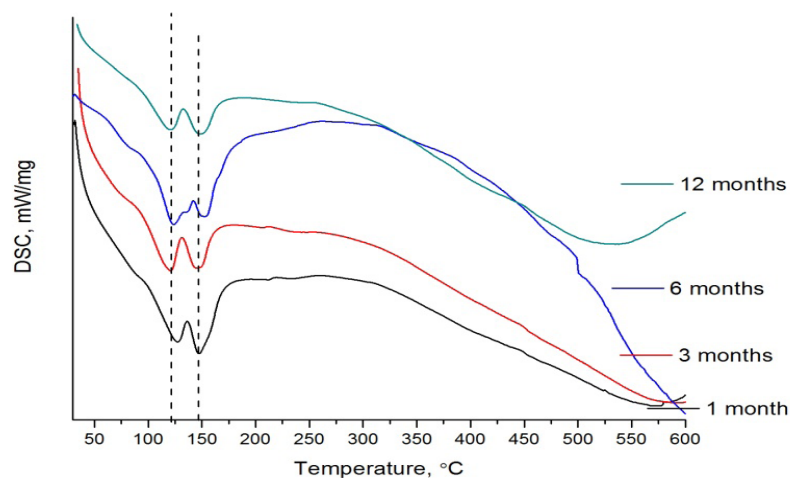


Fig. 13. DSC curves of D samples cured in Magnesium Chloride solution for 1, 3, 6 and 12 months.

the OPC content in SSC pastes as the peaks of cement D are more pronounced than that of cement B. These results are in a good agreement with our FTIR spectroscopy deductions.

### Conclusion

The main conclusions of the present investigation are summarized as follows:

- Supersulphated cement (SSC) pastes showed a higher durability to magnesium chloride solution due to several factors including the lack of calcium hydroxide which is consumed during hydration of slag in hardened pastes.
- The durability of the SSC pastes is shown as an increase in the compressive strength values and the bulk density also as a decrease in the apparent porosity values.
- The percentage of the OPC included in the SSC plays an important role in the activation of slag and producing hydration products that fill the open pores and increase the bulk density and the compressive strength and thus increasing the durability.
- XRD and FTIR techniques showed that the main hydration products are ettringite, CSH and gypsum.
- Detection of the hydration products using thermal analysis tools showed a shift of the peaks towards higher temperature as the alkaline activator percentage increase as well as the hydration time increases.

### References

1. Monteiro P. *Concrete: Microstructure, Properties, and Materials*. McGraw-Hill Publishing (2006).
2. Bastidas D.M., Fernández-Jiménez A., Palomo A. and González J.A., A study on the passive state stability of steel embedded in activated fly ash mortars. *Corrosion Science*, **50**(4), 1058-1065 (2008).
3. Broomfield J.P. *Corrosion of Steel in Concrete: Understanding, Investigation and Repair* CRC Press, (2006).
4. Chung L., Jay J.H. and Yi S.T., Bond strength prediction for reinforced concrete members with highly corroded reinforcing bars. *Cement and Concrete Composites*, **30** (7), 603-611 (2008).
5. Meira G.R., Andrade C., Padaratzv I.J., Alonso C. and Borba J.C., Chloride penetration into concrete structures in the marine atmosphere zone - relationship between deposition of chlorides on the wet candle and chlorides accumulated into concrete. *Cement and Concrete Composites*, **29** (9), 667-676 (2007).
6. Lambert P., Page C. L., and Short N. R., Pore solution chemistry of the hydrated system tricalcium silicate/sodium chloride/water. *Cement and Concrete Research*, **15** (4), 680-675 (1985).
7. Arya C. and Xu Y., Effect of cement type on chloride binding and corrosion of steel in concrete. *Cement and Concrete Research*, **25**(4), 893-902 (1995).

8. Choi Y.S., Kim J.G. and Lee K.M., Corrosion behavior of steel bar embedded in fly ash concrete. *Corrosion Science*, **48** (7), 1733-1745 (2006).
9. Song, H.W. and Saraswathy, V., Studies on the corrosion resistance of reinforced steel in concrete with ground granulated blast-furnace slag. An overview. *Journal of Hazardous Materials*, **138** (2), 226-233 (2006).
10. Aprianti, E., Shafiqh, P., Bahri, S., Farahani, J.N., Supplementary cementitious materials origin from agricultural wastes - a review. *Construction and Building Materials*, **74**, 176-187c (2015).
11. Juenger, M.C.G., Winnefeld, F., Provis, J.L. and Ideker, J.H., Advances in alternative cementitious binders. *Cement and Concrete Research*, **41**, 1232-1243 (2011).
12. Damtoft, J.S., Lukasik, J., Herfort, D., Sorrentino D. and Gartner, E.M., Sustainable development and climate change initiatives. *Cement and Concrete Research*, **38** (2), 115-12 (2008).
13. Fernández-Jimenez, A. and Puertas, F., Effect of activator mix on the hydration and strength behavior of alkali-activated slag cements. *Advances in Cement Research*, **15** (3), 129-136 (2003).
14. Fernández-Jiménez, A., Miranda, J.M., González, J.A. and Palomo, A. Steel passive state stability in activated fly ash mortars. *Materiales de Construcción*, **60** (300), 51-65 (2010)
15. Puertas, F., Gil-Maroto, A., Palacios, M. and Amat, T., Alkali-activated slag mortars reinforced with a glass fibre. Performance and properties. *Materiales de Construcción*, **56** (283), 79-90 (2006).
16. Roy, D.M., Jiang, W., and Silsbee, M.R., Chloride diffusion in ordinary, blended, and alkali-activated cement pastes and its relation to other properties. *Cement and Concrete Research*, **30** (12), 1879-1884 (2000).
17. Taylor, H.F.W. "Cement Chemistry" Thomas Telford (1997).
18. Hewlett, P. C. "Lea's Chemistry of Cement and Concrete" Elsevier (2003).
19. ASTM C109, Standard Test Method for Compressive Strength of Hydraulic Cement Mortars (Cube Specimens), ASTM International, (2002).
20. Gu, K., Jin, F., Al-Tabbaa, A., and Shi, B., Activation of ground granulated blast furnace slag by using calcined dolomite. *Construction and Building Materials*, **68**, 252-258 (2014).
21. Gastaldi, D., Canonico, F., Boccaleri, E., Ettringite and calcium sulfoaluminate cement: investigation of water content by near-infrared spectroscopy. *Journal of Materials Science*, **44** (21), 5788-5794 (2009)
22. Bensted, J. and Varma, S.P., Studies of ettringite and its derivatives. *Cement Technology*, **2** (3), 73-77 (1971)
23. Collier, N. C. C., Li X., Bai Y., and Milestone N. B. B. The effect of sulfate activation on the early age hydration of BFS: PC composite cement. *Journal of Nuclear Materials*, 464, 128-134 (2015).
24. Gruskovnjak, A., Lothenbach, B., Winnefeld, F., Figi, R., Ko, S. C., Adler, M., and Mäder, U., Hydration mechanisms of super sulphated slag cement. *Cement and Concrete Research*, **38** (7), 983-992 (2008).

### دراسة مقاومة العجائن الأسمنتية فائقة المقاومة للكبريتات المنشطة بالاسمنت البورتلاندي لمحلول كلوريد المغنسيوم

أحمد عبد الحليم حجازي<sup>١</sup>، عبد العزيز أحمد خليل<sup>١</sup>، السيد علي الألفي<sup>١</sup>، محمد فتحي الشحات<sup>٢</sup>  
<sup>١</sup>قسم الحرارية والسيراميك ومواد البناء - المركز القومي للبحوث - القاهرة - مصر.  
<sup>٢</sup>قسم الكيمياء - كلية العلوم - جامعة عين شمس - القاهرة - مصر.

تبحث هذه الدراسة تأثير الكلوريدات على الخواص الفيزيوميكانيكية للأسمنت فائق المقاومة للكبريتات الذي تم تحضيره باستخدام نسب مختلفة تتراوح ما بين ٢ إلى ١١٪ من الأسمنت البورتلاندي العادي الذي استخدم كمحفز قلوي. أشارت النتائج إلى أنه بعد غمر العينات التي تم تحضيرها في محلول كلوريد المغنسيوم تركيز ٤٪ لمدة تصل إلى ١٢ شهراً زادت قيم الكثافة الظاهرية بينما تناقصت قيم المسامية الظاهرية مع الوقت لكل خلطات الأسمنت فائق المقاومة للكبريتات بينما الخلطة المكونة من الأسمنت البورتلاندي العادي بدون أي إضافات كانت تعاني من ظهور تصدعات بعد ٣ أشهر فقط من الغمر. أظهرت نتائج مقاومة الانضغاط زيادة ملحوظة في جميع عينات الأسمنت فائق المقاومة للكبريتات التي تم غمرها في محلول كلوريد المغنسيوم حتى ١٢ شهراً وأظهرت مقاومة عالية لمحلول كلوريد المغنسيوم الذي يعتبر بيئة معادية للأسمنت.